

# Observations of equatorial mesospheric winds over Cariri (7.4° S) by a meteor radar and comparison with existing models

R. A. Buriti<sup>1,\*</sup>, W. K. Hocking<sup>2</sup>, P. P. Batista<sup>3</sup>, A. F. Medeiros<sup>1</sup>, and B. R. Clemesha<sup>3</sup>

<sup>1</sup>Departamento de Física, Universidade Federal de Campina Grande, Campina Grande, PB, 58109-970, Brazil

<sup>2</sup>Department of Physics and Astronomy, University of Western Ontario, London, Ontario, Canada

<sup>3</sup>Instituto Nacional de Pesquisas Espaciais (INPE), Sao Jose dos Campos, SP, Brazil

\*now at: Department of Physics and Astronomy, UWO, London, Canada

Received: 10 March 2006 – Revised: 19 October 2007 – Accepted: 17 December 2007 – Published: 26 March 2008

**Abstract.** Mesospheric winds observed with a meteor radar at Cariri (7.4° S, 36.5° W), Brazil, during the period of July 2004 to June 2005, show a clear semiannual oscillation known as the Mesospheric Semiannual Oscillation (MSAO), which maximizes in the zonal mean wind mainly at 82 km, with amplitude decreasing with height. Maximum westward winds for the MSAO occurred in March and September. The meridional wind, on the other hand, presented a clear annual variation maximizing in December. On average, the amplitude of the meridional MSAO was smaller than the zonal MSAO component. Comparison with models shows on occasions that there are significant differences between the observed winds and the CIRA (Cospar International Reference Atmosphere) and HWM93 (Horizontal Wind Model) models. In addition, diurnal and semidiurnal parameters were calculated and compared to the GSWM model. Other results observed during one year of data are presented in this work.

**Keywords.** Meteorology and atmospheric dynamics (General circulation; Middle atmosphere dynamics; Waves and tides)

## 1 Introduction

Routine observations of mesospheric wind in the equatorial region by meteor radar have become frequent since the beginning of this decade. At present, there are about 5 meteor radars performing continuous observations of mesospheric wind between 80 and 100 km in the equatorial regions. This is a starting point to diminish the observational deficiencies for this region. Between the 1970 and 1999, the main information about the Mesosphere and Lower Thermosphere (MLT) winds came from the medium and high frequency (MF/HF) radars which measure the winds between ~60 and

100 km (Manson et al., 1991), but most of these radars were installed outside the equatorial region. Observations by optical instruments on board rockets and satellites (e.g. Reed, 1965; Groves, 1972; Salby et al., 1984; Lieberman et al., 1993; Burrage et al., 1996; Garcia et al., 1997) also have contributed to the knowledge of the complex dynamics of the MLT in the equatorial region. However, a few measurements at a limited number of sites may not be fully representative of the full character of equatorial dynamics. Geographic location is a factor that must be considered. For example, some radars are located in the middle of, or close to, the oceans, for example, Ascension Island, UK (Pancheva et al., 2004), whereas others are located over land and in more convective regions. The Cariri radar is located 200 km east of the coast and 2500 km west of the Amazon region in Brazil, where tropical convection activity is strong (Taylor and Hapgood, 1988; Medeiros et al., 2005), and this location produces different results than radars located on islands.

The dynamics of the MLT in the equatorial region is quite different to mid-latitudes. The effect of the Coriolis force is small, resulting in waves and dynamics which are unique to this region. These unique waves can contribute to the Quasi-Biennial Oscillation (QBO) and Semi-Annual Oscillation (SAO) of the MLT winds (Hirota, 1978). The QBO and SAO, which are related to each other, are unique to the equatorial region and are attributed to momentum transport generated by planetary and gravity waves in the troposphere and stratosphere (Dunkerton, 1979; Garcia and Sassi, 1999).

Knowledge about diurnal and semidiurnal tides in the mesospheric region also increased considerably in the 1990's, following on-board measurements with HRDI and WINDII from the UARS satellite (e.g. McLandress et al., 1996). These oscillations are generated by thermal forcing when water vapor and ozone absorb radiation in the troposphere and stratosphere, respectively. Additionally, more realistic atmospheric parameters, such as better descriptions of energy and momentum dissipation process and nonlinear

Correspondence to: R. A. Buriti  
(rburiti@pesquisador.cnpq.br)

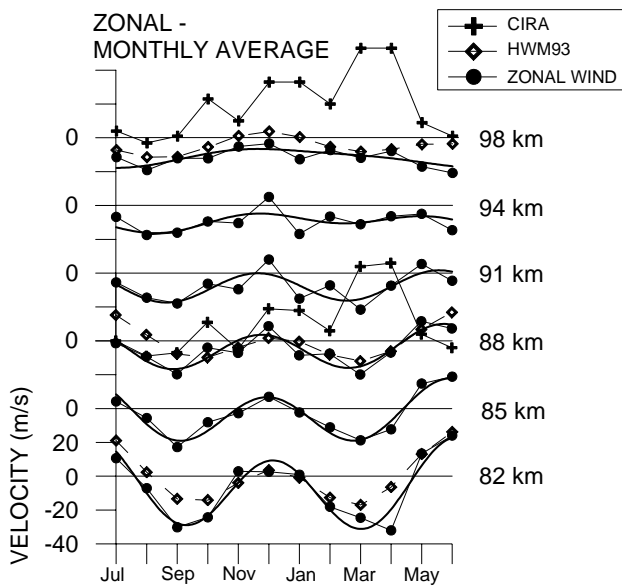


**Fig. 1.** Mean (monthly average) zonal wind at heights from 82 to 98 km between July 2004 and June 2005 observed at Cariri (solid circles). Thin lines represent the fitting of annual and semiannual oscillations. Open diamonds are the winds provided by HWM93 for Cariri at 82, 88 and 98 km. Solid crosses represent the winds given by CIRA model at 87.5 and 98 km.

interactions between tides, gravity and planetary waves as responsible (or not) for the semiannual oscillation, have been recently considered, producing better theoretical descriptions of the tides as a function of altitude, season and latitude (Geller et al., 1997; Forbes, 1982; McLandress, 2002a,b; Hagan et al., 2002; Hagan et al., 2003).

This paper concerns the analysis of one year of observation by meteor radar installed at Cariri ( $7.4^{\circ}$  S,  $36.5^{\circ}$  W; GMT Offset is  $-3$  h) in June 2004. We emphasize the mean zonal and meridional winds and the diurnal/semiannual oscillations. Comparisons with models are included where appropriate.

## 2 Instrumentation

The equipment used to observe winds in the mesosphere is an All-Sky Interferometric Meteor Radar called SKiYMET which uses an antenna array composed of a 2-element yagi antennas (5 in total) for reception and a 3-element yagi transmitting antenna. This particular SKiYMET operates at a frequency of 35.24 MHz and the output power is 12 KW peak. The radar measures the radial velocity by transmitted radiation scattered from meteor trails. The differences in phase of the signal received by each possible pairing of antennas identifies the location of the trail. The range is obtained by the delay between the transmitted and received signal. Zonal, meridional and vertical velocity components are determined by a least-squares fit to all the radial velocities measured in

a given time/height bin. Vertical velocities are normally very small and are ignored. The temporal and vertical resolutions of this radar are typically 1 h and 2–3 km, respectively. The Cariri radar is similar to the one installed in Cachoeira Paulista (Batista et al., 2004) and it is the third in operation in Brazil. Technical and acquisition details about this radar can be found in Hocking and Thayaparan (1997) and Hocking et al. (2001). This radar also measures the temperature at the height of meteor peak count rates but this parameter was not used in this work.

## 3 Mean zonal and meridional winds

The wind data obtained by the meteor radar were analyzed separately for the zonal and meridional components. This is standard practice for this kind of study. The data were subject to composite-day harmonic analyses, which produced mean winds as well as tidal amplitudes and phases for the diurnal, semiannual and terdiurnal oscillations. We will not discuss the terdiurnal component, but the other parameters will be discussed in the following sections.

### 3.1 Zonal mean winds

The monthly average zonal wind is basically westward, except during the summer and winter solstices when the wind is weakly eastward between 82 and 91–94 km. The presence of a semiannual oscillation (SAO) in the zonal wind, mainly between 82 and 91 km, is evident. At 98 km the zonal wind is completely westward. Data from HRDI, as well as an MF radar at Christmas Island, have shown similar behaviour (Garcia et al., 1997). Figure 1 shows the monthly mean zonal wind behavior from 4 July to 5 June. In this figure we included model wind calculations according to the HWM93 and CIRA models (Hedin et al., 1991, 1996; Fleming et al., 1990). Table 1 shows the quantitative estimates obtained by harmonic analyses of the amplitude and phase (month of maximum) for 6 (semiannual) and 12 (annual) months for the zonal and meridional average monthly wind. The values in parentheses are the errors. According to Table 1 and Fig. 1, the zonal semiannual amplitude is generally more important than the annual one. The ratio between semiannual and annual amplitudes is largest at 91 km, being about 8.0, but at 98 km the annual amplitude seems dominant. At 82 km the wind showed the largest semiannual amplitude, reaching 22.6 m/s, with a maximum westward intensity of about 31 m/s in September 2004 and March 2005. This amplitude decreases almost linearly by about 4.5 m/s for each 3 km of height from 82 to 94 km.

The semiannual oscillation has a downward phase shift with speed of about 16 km/month between 82 and 98 km of height. The time of maximum is near the beginning of November at 98 km and in the beginning of December 2004 at 82 km. We define the phase as starting on 1 July 2004,

**Table 1.** Wave parameters of zonal and meridional annual and semiannual winds above Cariri. Phase starts on 1 July 2004, which is taken as day 1 (one).

Zonal	Altitude (km)	82	85	88	91	94	98
Annual	DC (m/s)	-6.1 (2.2)	-3.4 (1.3)	-4.7 (1.7)	-8.0 (2.1)	-10.7 (1.9)	-12.2 (1.5)
	Amp. (m/s)	6.6 (0.1)	5.7 (1.8)	3.2 (2.5)	1.1 (2.9)	3.1 (2.7)	5.7 (2.1)
	Phase (month)	11.1 (0.5)	11.2 (0.3)	10.5 (0.8)	9.5 (2.8)	9.0 (0.9)	5.7 (0.4)
Semiannual	Amp. (m/s)	22.6 (3.1)	15.8 (1.8)	11.5 (2.5)	8.8 (2.9)	3.8 (2.7)	3.3 (2.1)
	Phase (month)	5.1 (0.1)	4.9 (0.1)	4.8 (0.2)	4.6 (0.3)	4.3 (0.7)	4.1 (0.6)
	Ratio	3.4	2.8	3.6	8.0	1.2	0.6
Meridional	Altitude (km)	82	85	88	91	94	98
Annual	DC (m/s)	-1.8 (1.0)	-3.0 (0.7)	-3.8 (0.6)	-4.7 (0.8)	-6.8 (1.1)	-10.0 (1.8)
	Amp. (m/s)	8.9 (1.4)	8.1 (1.0)	8.2 (0.9)	9.5 (1.1)	11.3 (1.6)	13.5 (2.5)
	Phase (month)	5.4 (0.3)	5.5 (0.2)	5.6 (0.2)	5.7 (0.2)	5.8 (0.3)	5.5 (0.4)
Semiannual	Amp. (m/s)	3.1 (1.4)	3.9 (1.0)	3.2 (0.9)	0.9 (1.1)	1.4 (1.6)	5.4 (2.5)
	Phase (month)	4.4 (0.5)	3.7 (0.3)	3.3 (0.3)	2.5 (1.2)	5.7 (1.0)	5.3 (0.4)
	Ratio	0.3	0.5	0.4	0.1	0.1	0.4

which is taken to be day 1 of month 1, so these dates correspond to the phases of 4.1 months and 5.1 months, respectively.

The annual amplitude of zonal wind, on the other hand, presents a minimum at 91 km and increases both above and below this altitude. The annual harmonic phase seems to move down, mainly between 85 and 98 km. Note that the amplitudes present a considerable error at 88–94 km, so it is necessary to avoid drawing conclusions about this component at this altitude.

### 3.2 Meridional mean winds

A southward wind is always present between July and September 2004 and from April to June 2005. A small northward flow, on the other hand, can be observed, from November 2004 to January 2005 (Fig. 2). In contrast to the zonal wind, the annual component of the meridional wind dominates, especially at 91 and 94 km, where the amplitude is about 10 times the semiannual one. These ratios are shown in the last line of the Table 1. The annual peak intensity, according to harmonic analysis, is located in December 2004. The maximum and minimum annual amplitudes are about 13.5 m/s at 98 km and ~8.1 m/s at 85–88 km, respectively. The meridional annual harmonic phase shows very little variation with height. Our best estimate is that it moves down with a velocity of 36 km/month, but this calculation has a large error, and the wave can almost be considered as evanescent. This value was obtained considering the range of altitude between 82 and 94 km where the variation of the phase is monotonic. There is a jump in the semiannual phase between 91 and 94 km, but it is worth commenting that these regions present the smallest values of semiannual amplitude and the errors are larger.

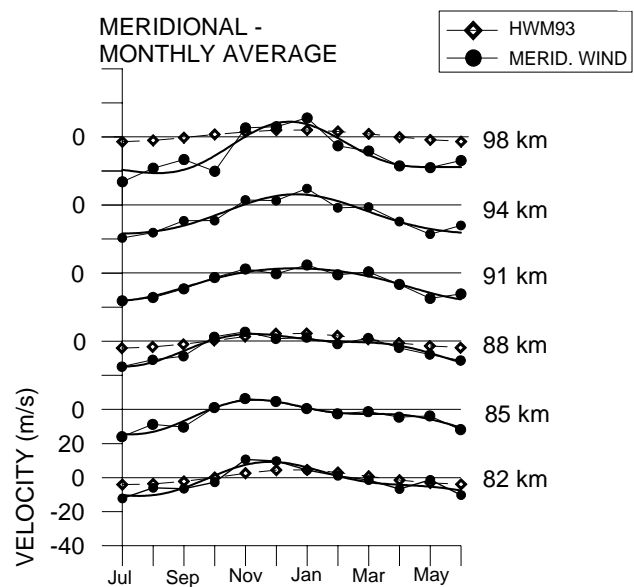


**Fig. 2.** Mean (monthly average) meridional wind at heights from 82 to 98 km between July 2004 and June 2005 observed at Cariri (solid circles). Thin lines represent the fitting of annual and semiannual oscillations. Open diamonds are the winds provided by HWM93 for Cariri at 82, 88 and 98 km.

The RMS mean meridional and zonal winds, on average, were 37 m/s and 30 m/s, respectively. This means that the meridional wind variability is ~23% higher than zonal wind during these 12 months of observation. This can be compared with the data for Cachoeira Paulista (Batista et al., 2004), where the variability of the zonal wind is much higher than that of the meridional one. That site is located at 22.7° S and 45° W.

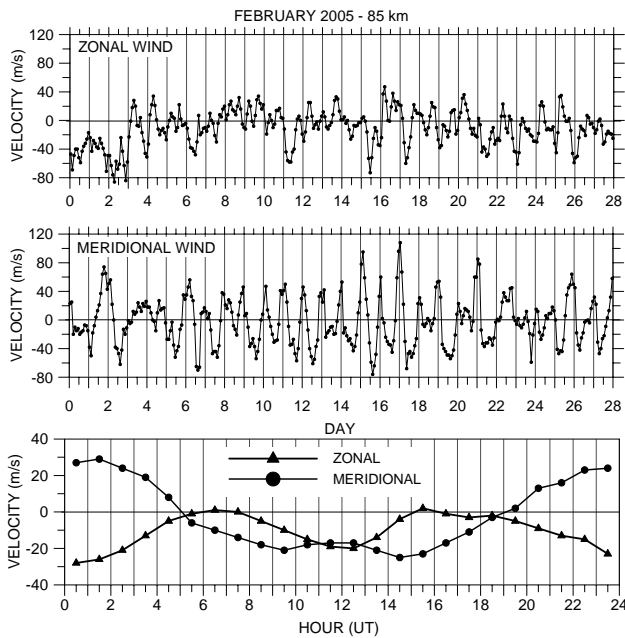


**Fig. 3.** The two upper plots show the 85-km zonal and meridional winds each 2 h from 1 to 28 February. Bottom plot shows the zonal (solid triangles) and meridional (solid circles) hourly winds for a composite day from 00:50 to 23:50 UT at same altitude.

A comparison between the observed data at Cariri and other sites, and the winds provided by HWM93 and CIRA is present in the Discussion section. Briefly, we can say that HWM93 describes qualitatively well our observation, especially during the summer season. On the other hand, CIRA seems to be far from describing the data from Cariri, especially at the upper altitudes. The flow to the west, observed in March/April, is not predicted by CIRA. This may be due to the fact that the CIRA equatorial data were based on limited data sets, since few reliable equatorial instruments were available when CIRA was prepared. The CIRA does not present a model of the mean meridional wind.

#### 4 Diurnal and semidiurnal tides

The amplitudes and phases of the semidiurnal and diurnal oscillations present in the wind data from Cariri were obtained using standard least-squares fitting techniques. We have adopted the same procedure as Hocking (2001), who binned all meteors for a specific month solely according to time of day (“composite day”). The final result shows the hourly behavior of the wind during the composite day at specific heights. It is worth noting that each hour of the composite day contains over 5000 points which makes the errors generally low. The two upper plots of Fig. 3 show the two-hourly zonal and meridional winds from 1 to 28 February as an example. From these plots, composite day plots of

the wind (bottom plot of Fig. 3) could be obtained. Following this, harmonic fits to the composite day data allowed the amplitude and phase for diurnal, semidiurnal and terdiurnal tides (not discussed in this work) of the wind measured by the meteor radar to be found. The procedure used to calculate the errors, which include a random error and intrinsic geophysical variability, is described by Bevington (1969), and has been applied by multiple authors in the past (Hocking and Hocking, 2002; Wu et al., 1995; Vincent et al., 1988, among others). Weightings for each hour were determined from inverse variances, and then the procedures described by Bevington (chapters 8 and 11, and especially pages 242–246) were used to calculate the standard deviation of the diurnal and semidiurnal amplitudes and phases of every month studied in this work. The errors were, in general, less than 10% for amplitudes and less than one hour for phases.

##### 4.1 Diurnal oscillation

The results for the diurnal oscillation in amplitudes and phases according to the least-squares fitting can be seen in Figs. 4 and 5, respectively. The amplitudes of diurnal oscillation for zonal and meridional winds are shown in Fig. 4a and b, respectively. The horizontal lines represent the value 0 (zero) at the respective altitude. A dominant semiannual oscillation of the zonal diurnal amplitude, mainly between 91 and 98 km, with maximum at the equinoxes, is evident. The diurnal oscillation has amplitudes varying between 1 and 38 m/s, with an average of  $11.9 \pm 7.8$  m/s in the range of 82 and 98 km. The mean amplitude from July 2004 to June 2005 at 82 km was 6.8 m/s and at 98 km this value was about 20 m/s, an increase of almost 3 times. November was a unique month in that the amplitude decreased rather than increased, by about 0.7 m/s/km between 85 and 98 km.

The meridional diurnal amplitudes (Fig. 4b) presented a clear oscillation of a 6-month period, with peaks in September–October and March–April in the range of an altitude from 85 to 94 km. At 82 and 98 km, this oscillation seems to disappear. The diurnal oscillation had amplitudes between 5 and 43.5 m/s, with an average of  $23.7 \pm 9.0$  m/s in the range of 82 and 98 km. This is almost twice the value of the zonal diurnal amplitude. The equinoctial months showed behaviour similar to the average, in other words, they had a peak of amplitude around 91 km. In May, June and July, the amplitudes increased with height while in November–January they were practically constant. According to the tidal theory (Chapman and Lindzen, 1970; Forbes, 1982), at  $7.5^\circ$  S, the meridional diurnal tide (1,1) is expected to be larger (by about 50%) than the zonal one.

In general, the observed diurnal amplitudes for zonal and meridional wind show good agreement with the Global Scale Wave Model (GSWM-02) (Hagan et al., 2002, 2003) but a pronounced difference between observations and the model can be seen in the meridional amplitude for October at 85 and 94 km and in the zonal component at 94 km

for April (Fig. 4a and b). A comprehensive description of this model can be found at the website of the High Altitude Observatory (HAO) of the National Center for Atmospheric Research, in Colorado (<http://web.hao.ucar.edu/public/research/tiso/gswm/gswm.html>).

The phase (hour of maximum) for diurnal oscillation in zonal and meridional wind for all 12 months is shown in Fig. 5. Because the amplitudes of zonal diurnal component throughout the months are small at 82 km, the phase calculated for this height is not shown in Fig. 5. The phase behavior was quite different for the two components. The zonal phases between 85 and 98 km fluctuated between 18:30 LT and 13:50 LT. Between 85 and 91 km, the phase presented 2 distinct peaks, one in September–October and the other in February–April. In November the phases of most of the heights seemed to converge at 21:45 LT, on average, so that the tide was close to evanescent in that month. The meridional phase varies smoothly with height. For example, at 98 km, the average phase during the year is 09:20 LT and changes by  $\sim 3$  h for each 3 km from 82 to 98 km. The phase has two minima and varies smoothly throughout the year, except at 98 km. We may also use the phase variation with height to determine the vertical wavelength. In the case of the zonal components, phases for the zonal wind did not vary smoothly between the heights in some specific months, and it was rare to be able to fit them to a straight line. Consequently, the calculation of vertical wavelength was not precise and/or was not possible. This problem did not occur with meridional vertical wavelength calculation. In Fig. 5, some months have the phases that are very close to each other, so that the wavelength is large, while for January 2005 the phases are widely spaced, and the wavelength is small. Figure 6 shows the plots in more detail. On the other hand, in the case of the meridional component the classical (1,1) mode seems to dominate compared with all other modes at this latitude ( $7.4^\circ$  S).

In order to estimate the vertical wavelength of the diurnal tide, we have plotted in Fig. 6 the phase of zonal and meridional components from January to April as a function of altitude. Good fit (when R-squared or coefficient of determination is great than 0.81) is observed for the meridional phase, indicating a constant vertical wavelength throughout the whole height interval. In contrast, for the zonal phase, a good fit is obtained only for limited heights. In every month analyzed, the zonal diurnal oscillation led the meridional, except at 82–85 km, where, during some months, the opposite occurred. Physically, this means that the wave, which is assumed to propagate upward, gives rise to a wind vector which rotates anticlockwise with height looking from the top. This is expected for the Southern Hemisphere tide (Gill, 1982; Vincent, 1984).

The vertical wavelength of the diurnal oscillation of zonal and meridional wind as a function of month is showed in Fig. 7. The mean wavelength of the meridional wind, not considering July 2004, is  $23.8 \pm 2.6$  km. Tidal theory estimates a wavelength of 25 km for the mode (1,1) in the

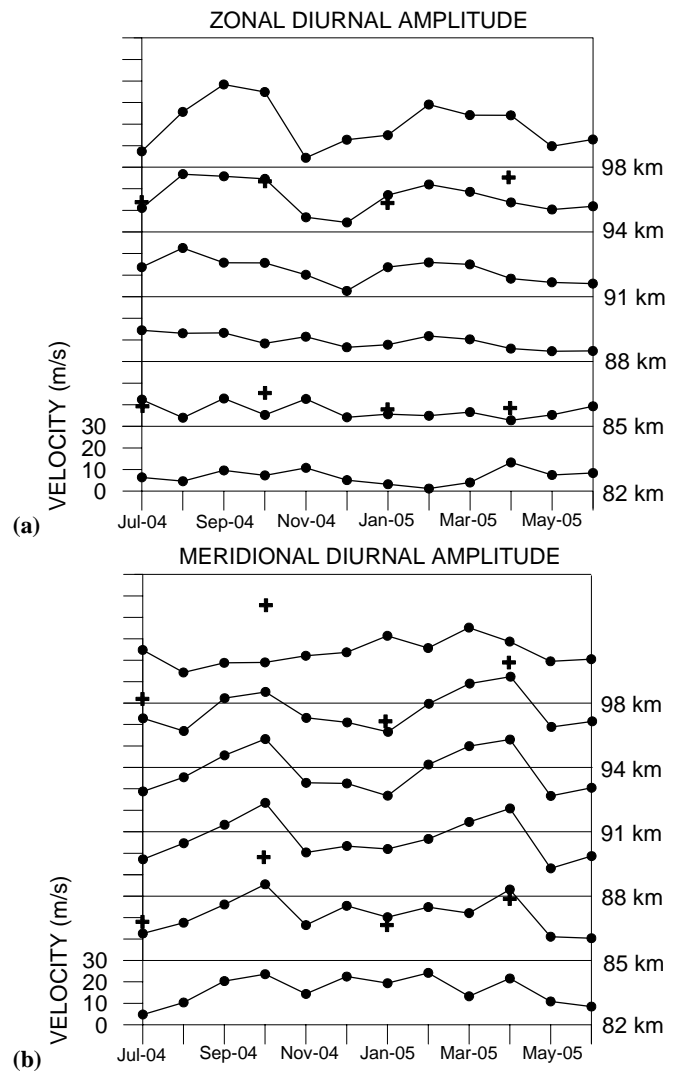


**Fig. 4.** Zonal (a) and Meridional (b) amplitude of the diurnal tide. Each horizontal line represents the value 0 (zero) at the respective height. The symbol (+) represents the amplitude provided by the model GSWM02 at  $\sim 86$  and  $\sim 94$  km.

absence of dissipative mechanisms (Forbes, 1982). The vertical wavelength of the zonal wind varied more than the meridional one, but in March and April, they are very similar.

The zonal phase for December is not linear with height, and the zonal phase in June was almost constant with measuring height. Therefore, in these two cases it was not possible to estimate the vertical wavelength. As for the zonal diurnal phase, the presence of other modes of propagation will complicate the determination of wavelength. It is worth commenting that the mean R-squared value for phase fitting of the diurnal meridional was 0.99.

A comparison of the GSWM-02 model with Cariri data can be seen in Fig. 8. The figure shows the observed (O) and model (M) diurnal zonal and meridional phases in January,

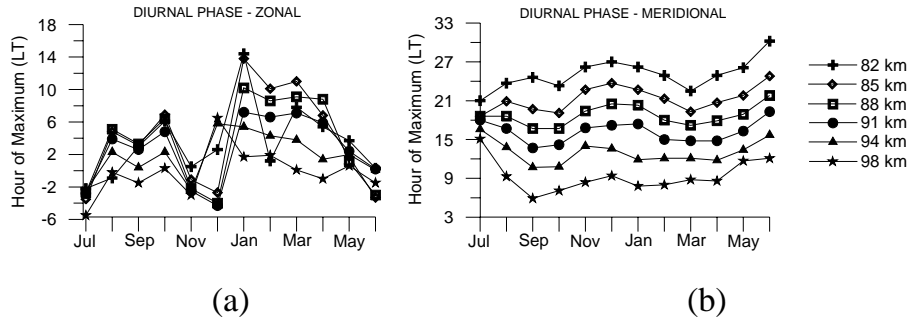


**Fig. 5.** Hour of maximum (Local Time) for zonal (a) and meridional (b) diurnal oscillations from July 2004 to June 2005.

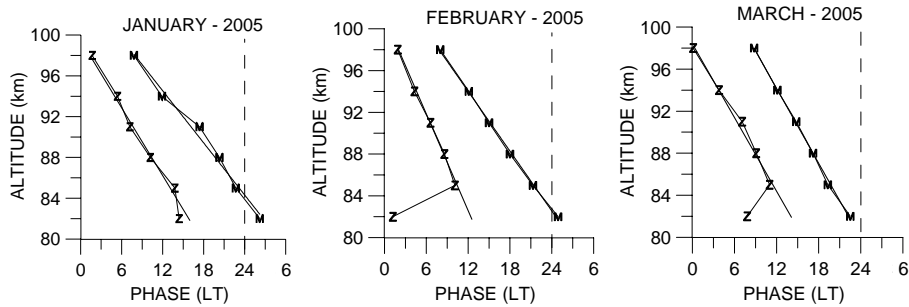


**Fig. 6.** Phase of zonal (Z) and meridional (M) diurnal tide from January 2005 to March 2005. The thick lines indicate the best fit used to calculate the vertical wavelength.

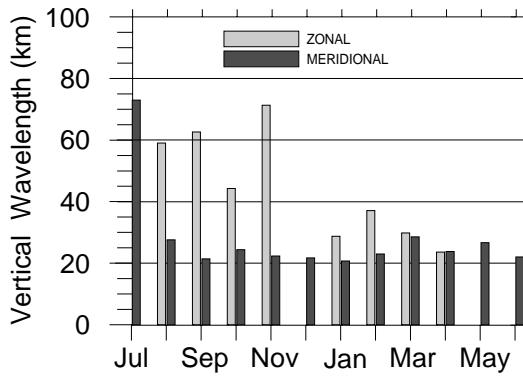


**Fig. 7.** Vertical wavelength of diurnal oscillation for zonal and meridional components from July 2004 to June 2005.

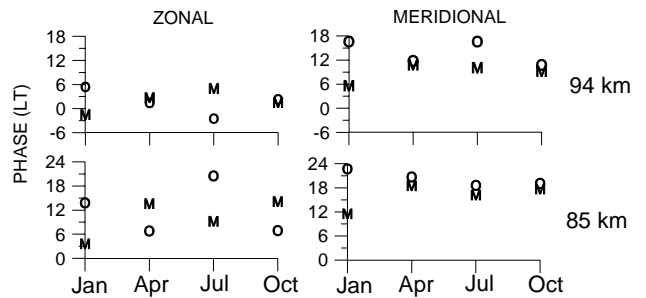


**Fig. 8.** Comparison between observed (O) and GSWM model (M) phases at Cariri at 82 and 94 km in January, April, July and October.

April, July and October at  $\sim 85$  and  $\sim 94$  km. The zonal component seems to have a good agreement at 94 km, especially for April and October. At 85 km, the difference between the observation and GSWM-02 in April and October is about 6 h. According to the model, the zonal phase leads the meridional one at 85 and 94 km throughout the year by about 6.7 h, but the data show that the meridional leads the zonal wind in both solstices. The observed and model meridional components do not match in January at 85 km and in January and July at 94 km. In April and October, the difference between them is 0.8 h and 1.2 h, respectively.

#### 4.2 Semidiurnal oscillation

The semidiurnal oscillation was also investigated in this work. The behavior of the amplitude during 12 months can be seen in Fig. 9. The average zonal semidiurnal amplitude was  $5.8 \pm 3.4$  m/s with values between 1 and 18 m/s. November generally presented the highest value for the amplitude, about 12 m/s, while July 2004 and June 2005 had the lowest values,  $\sim 2.7$  m/s.

On average, a meridional semidiurnal oscillation of  $\sim 15.0 \pm 7.0$  m/s was observed; this is 2.6 times higher than the zonal one. The amplitude increased with height, by about 2.2 m/s for each 3 km, but shows an interesting behavior throughout the year. Between October 2004 (20 m/s)

and February (4.0 m/s), the amplitude decreased by about 4.1 m/s per month and then increased abruptly to 20 m/s in March 2005.

Similarly to the zonal diurnal phase, the semidiurnal phases (Fig. 10a) did not have a monotonic progression with time and height, indicating a sum of different modes with different amplitudes and an upward or downward propagation in the range between 82 and 98 km. Another point we must consider is the possibility of the presence of non-migrating tides. For this reason the phases for some months could not be fitted to a straight line throughout the whole data interval, especially for the zonal component. On the other hand, the meridional semidiurnal phase presented clear downward phase propagation between September and April. According to Fig. 10b, there was a tendency for an annual variation of the phase. The phase during summer solstice (December) was, on average, 04:00 LT (16:00 LT) while during winter (June/July) it was at around 10:00 LT (22:00 LT).

The vertical wavelength for the zonal and meridional semidiurnal oscillations was calculated in a similar manner to that for the diurnal one. The results are shown in Fig. 11. The zonal wavelength in July is negative which means upward phase propagation. The mean zonal vertical wavelength, not including July 2005, was  $49 \pm 16$  km while the meridional was  $54 \pm 24$  km. November was the only month when the zonal and meridional vertical wavelengths were similar, about 50 km. According to classical tidal theory, a vertical wavelength of about 50 km is typical of (2,4) modes while the (2,3) mode has a vertical wavelength around 80 km. Vertical wavelengths above 80 km could be attributed to evanescent waves or superposition of multiple tidal modes.

Figure 12 shows the observed (O) and GSWM model (M) values of the semidiurnal phases. In general, there is a good agreement between them, except for the zonal phase at 85 km in April and October, where the difference between observed and GSWM was around 5 h. The meridional phase at 94 km, also presented a significant difference of 5 h in January and October.

### 5 Spectral analysis

In order to investigate the presence of oscillations in the wind observed at Cariri throughout a year we obtained the rotary spectra over 12 months, from July 2004 to June 2005. In Fig. 13, we have plotted the running spectra for 3 specific heights, namely 82, 91 and 98 km. This technique consist basically in obtaining the Fourier transform of a length of data, called a window, and then moving this window forward in time along the principal series. We used 20 days (480 h) for the window length and moved this window in steps of 2 days (48 h). The process is repeated until all data (~365 days) have been analyzed. This technique is described in, e.g. Hocking (2001).

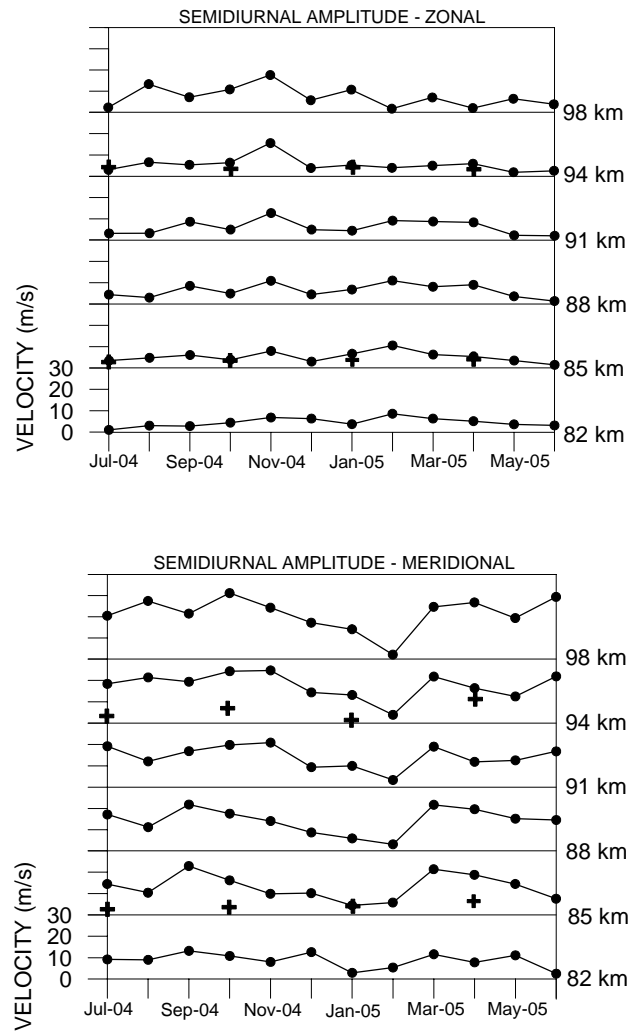


**Fig. 9.** Zonal (a) and meridional (b) amplitude of 12-h tide. Each horizontal line represents the value 0 (zero) at the respective height. The symbol (+) represents the amplitude calculated by the model GSWM at 82 and 94 km.

Briefly, in a rotary spectrum, each individual spectral line in frequency space represents a rotating vector in real space, where the rotating vector is obtained from two orthogonal times series (in this case, the zonal and meridional components). The sense of rotation (clockwise or anticlockwise) defines whether the spectral line is negative or positive. In other words, the horizontal mesospheric wind can be represented by a complex vector  $V(z)=u(z)+iv(z)$ , where  $u$  and  $v$  represent the zonal and meridional wind as a function of time at a specific height  $z$ . Because a complex number can be written as a function of  $\exp(\pm i2\pi ft)$ , the wind can be described as a combination of positive (anticlockwise) and negative frequencies (clockwise), each with their own respective amplitudes (O'Brien and Pillsbury, 1974; Vincent, 1984). The parameter  $f$  is the frequency of oscillation of

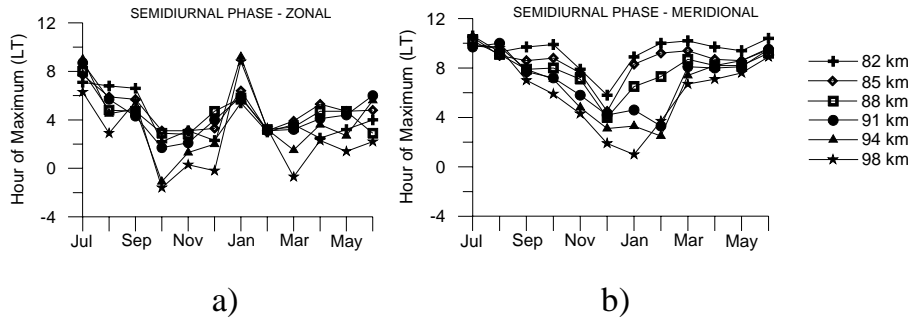


Fig. 10. Hour of maximum (phase) for zonal (a) and meridional (b) semidiurnal oscillations from July 2004 to June 2005.

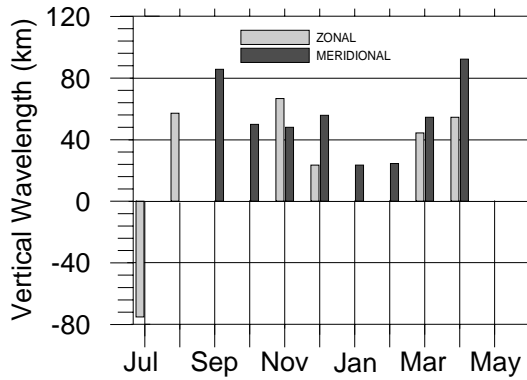


Fig. 11. Vertical wavelength of semidiurnal oscillation for zonal and meridional components from July 2004 to June 2005.

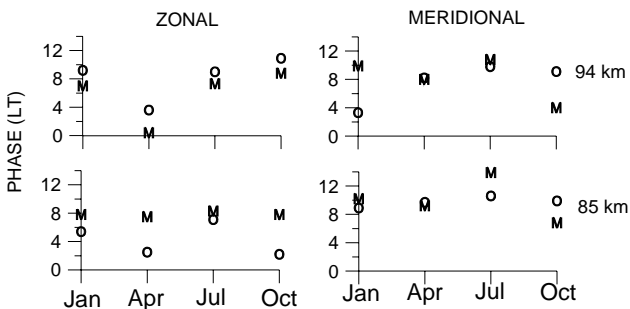
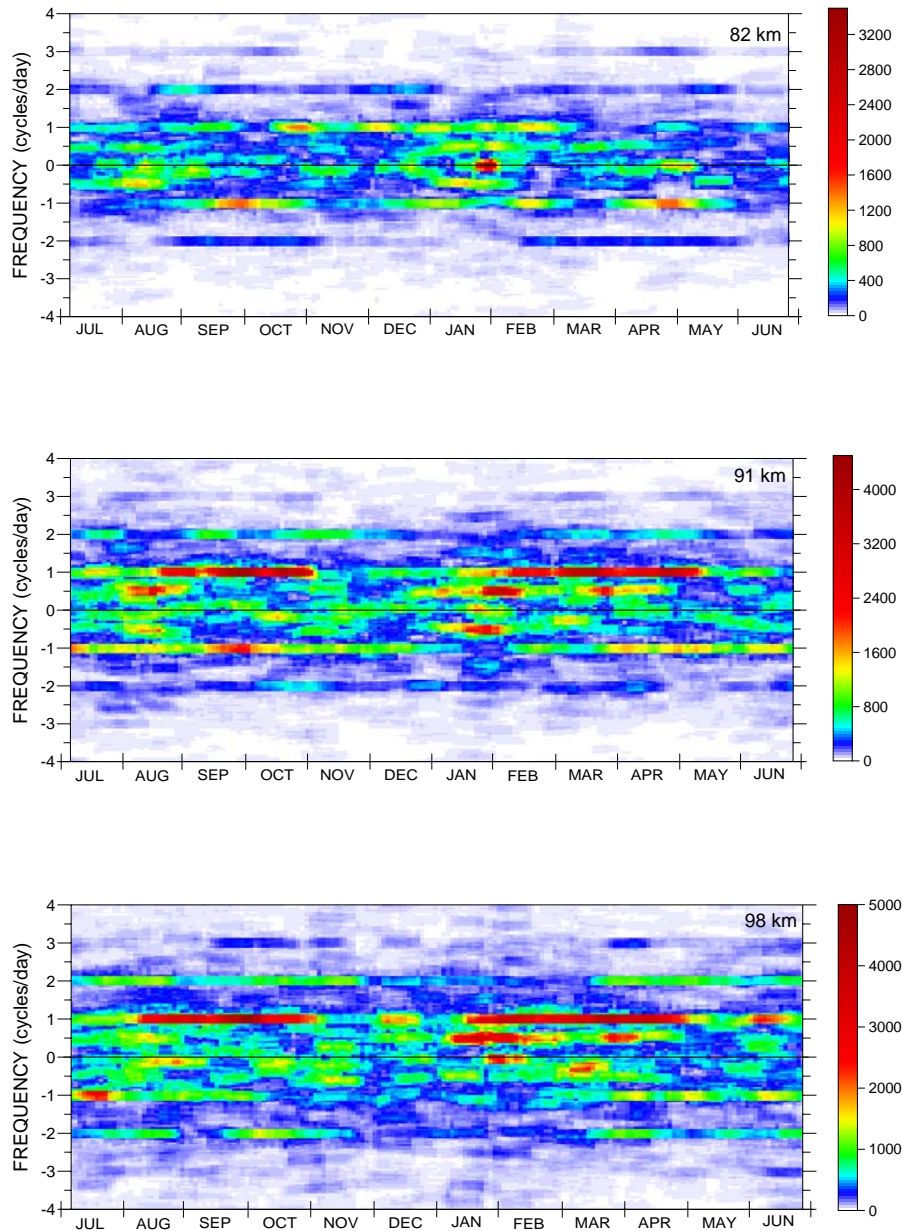


Fig. 12. Same as Fig. 8, but for the semidiurnal phase.

the wind. In the Southern Hemisphere, an upward wave will give rise to a wind vector rotating anticlockwise with increasing height. This means that the zonal wind leads the meridional wind. If the vector rotates clockwise, it means the wave is moving downward and the meridional wind leads the zonal one. The spectral density is related to the amplitude of the component (negative or positive) and the width of the peak relates to the variance of the frequency. If the spectrum presents 2 waves of similar frequency but different spectral density, the wave will rotate according to the larger spectral

density, and the rotation hodograph will be an ellipse. For example: if the power density of the negative frequency is larger than the positive one, then the wave rotates clockwise. If both have the same density, this wave propagates, upward or downward, like a linearly polarized wave.

Figure 13 shows clearly the presence of a semidiurnal and diurnal oscillation as well as a 2-day wave in both positive and negative frequencies. The plots show that, in general, the anticlockwise component is dominant, indicating that the propagation of tides and the 2-day waves are basically upward. At 82 km (Fig. 13a) the wave activity of both diurnal and semidiurnal tides, as well as for the 2-day wave, is less than at 91 and 98 km. The diurnal tide is present at both positive and negative frequencies. In September/October and April/May the PSD is stronger at negative frequencies, so the clockwise rotation is more important and a downward wave with a period of 1 day prevailed. Between October and March, it seems that upward propagation is more significant. In February the negative and positive frequencies seems to compete with each other, producing a linearly polarized tide. The semidiurnal component is weaker, but a clear seasonal activity is present at negative frequencies. Waves of 8 h (terdiurnal tides) are present only at positive frequencies in September/October and April/May. The 2-day wave activity is present at negative and positive frequencies but in December this wave seems to rise until February when clockwise rotation ceases. At 91 km the diurnal tidal activity is present throughout the year, but it is possible to note a clear seasonal behavior, with positive frequencies statistically more significant than the negative ones. This indicates that the diurnal tides are predominantly an anticlockwise rotation, mainly in the spring and fall equinoxes. In January, the rotation is practically anticlockwise because the negative frequency in the rotary spectrum vanishes. The semidiurnal oscillation at positive frequencies, similar to diurnal one, is also not present during all the months. The altitude of 98 km presents, similar to 91 km, predominantly anticlockwise rotation with strong seasonal behavior. But the clockwise rotation seems to decrease its amplitude mainly from October to February. The semidiurnal oscillation is strong between



**Fig. 13.** Running power spectrum of the wind at Cariri from July 2004 to June 2005 at 82 km (a), 91 km (b) and 98 km (c). The colors represent the power spectra density ( $\text{m}^2\text{s}^{-2}\text{day}$ ).

July and November 2004 and between March and June 2005. From July to November, the 2-day wave is not well defined, which makes it difficult to report about this wave in the period of observation. It is present between December and April with peaks in January/February and March/April in the positive frequency region.

## 6 Discussion

We have presented some results about winds observed at Cariri during the period between July 2004 and June 2005. The results include mean zonal and meridional winds, zonal and meridional amplitude and the phase of the diurnal and semidiurnal tides, as well as the distribution of occurrence of some important oscillations throughout 1 yr of data. The wind calculated by the empirical Horizontal Wind Model 93 (HWM93) for Cariri was compared to the observed wind at Cariri. This model is based on wind measured by satellites

(AE-E and DE-2), ground-based incoherent scatter radar, Fabry-Perot interferometers and MF-Meteor data. For the zonal wind, the model reproduces qualitatively very well the observed data but the magnitudes are very different. The ratio between the observed and model values is about a factor of 2, mainly at 82 km in the range July–September and April (Equinox). The agreements are better in other months. The meridional wind at 82 km presents a good agreement with the model but at heights of 88 and 98 km a large difference between the model and Cariri data are presented, except for summer when this difference is small.

The zonal winds observed at Cariri were also compared to the COSPAR International Reference Atmosphere (CIRA) model at 87.5 and 98 km. CIRA is identical to the Mass-Spectrometer-Incoherent-Scatter (MSIS) for altitudes above  $\sim 100$  km. Between 0 and 120 km of altitude, CIRA-86 consists of tables of zonal wind (monthly mean) and temperature from  $80^\circ$  S to  $80^\circ$  N, generated according to ground-based and Nimbus 5, 6 and 7 satellites measurements (Oort, 1983; Labitzke et al., 1985). Because the wind model data had a latitudinal resolution of 10 degrees, a simple interpolation between  $0^\circ$  and  $10^\circ$  S was made to calculate the wind at  $7.5^\circ$  S (latitude of Cariri). Data from equatorial sites were also limited in quantity and quality at the time that CIRA was made. The difference between the observed and model values is large, mainly at 98 km. In March and April, the difference between CIRA and Cariri is about 60 m/s. There seems to be in good agreement in the winter season at 88 km. This model does not predict the semiannual oscillation clearly observed at Cariri. The meridional wind is also not presented by CIRA.

The observation of a semiannual oscillation (SAO) in the mean zonal wind at mesospheric heights (MSAO) was reported, for the first time, by Reed (1966), using rocket-sonde observations. Groves (1972) also identified it near the mesopause using rocket and radar wind data. Published results to date suggest that the semiannual oscillation presents two maxima in amplitude, one near the mesopause and the other near the stratopause, with a minimum near 64 km. The times when the amplitudes are maxima are nearly in antiphase (Hirota, 1978), which can be explained by selective transmission of vertically propagation gravity and ultra-fast Kelvin waves through the SAO in the stratospheric (SSAO) winds (Dunkerton, 1982). With regard to our own data, we do not have data below 82 km, so cannot confirm the existence of a minimum at 64 km altitude. At our latitude the mesopause is at typically 95–98 km, which is close to our maximum height of observation. We can learn more by examining the results from stations at similar latitudes but different longitudes. We are aware of two stations with similar equatorial latitudes, namely Tirunelveli ( $8.7^\circ$  N,  $77.8^\circ$  E) and Christmas Island ( $2^\circ$  N,  $157^\circ$  W) at which MSAO studies have been carried out (Rajaram and Gurubaran, 1998; Vincent, 1993). The campaign at Tirunelveli was made between July 1994 and June 1995, and the one at Christmas

Island was made between January 1990 and June 1991, and these studies revealed maxima velocity amplitudes of 23 and 20 m/s, respectively, peaking at 84–86 km. These values are quite comparable to our own. Burrage et al. (1996) used 3 yr of data from the High Resolution Doppler Imager (HRDI) on the Upper Atmospheric Satellite (UARS) to study the MSAO, and reported an amplitude maximizing at 35 m/s near 82 km in the equatorial region. They found the maximum amplitude over Cariri to be close to 30 m/s. Hence our measured amplitudes are consistent with these other studies.

In contrast to our results, Rajaram and Gurubaran (1998) and Vincent (1993), who reported wind analyses of data observed over Christmas Island, did not observe a downward semiannual phase propagation in the mean zonal wind in the range 82 to 98 km altitude. Burrage et al. (1996), on the other hand, found a phase shift of about  $-15$  km/month above 80 km, which is very close to our results ( $-16$  km/month). Our observations are similar to those presented by Rajaram and Gurubaran (1998) for the months between July 1994 and June 1995, with data from Tirunelveli. Our observation of the mean meridional wind is also similar to that reported by Rajaram and Gurubaran (1998), especially if we consider wind data from July 1994 to June 1996. We must comment that MSAO did not present a clear seasonal asymmetry. Many researchers (e.g. Garcia et al., 1997) have reported about asymmetry in the MSAO ( $\sim 80$  km of altitude) westward between both equinoxes in the Ascension Island ( $7.6^\circ$  S). According to Burrage et al. (1996) this asymmetry can be attributed to a combination of MSAO with different annual variations in both hemispheres.

The amplitudes of the zonal and meridional diurnal oscillation have been compared with the GSWM amplitudes at 82.1 and 94.6 km in January, April, July and October. There is an excellent agreement between model and observed amplitude for the zonal component, except for January at 94 km, when the difference is almost a factor of 4. With regard to the meridional component, we could say that the model at 82 and 94.6 km does not match very well with the observed amplitude. The difference between the model and observed data in October was about 50% at 82 and 94 km. Data from Jakarta, ( $6^\circ$  S,  $109^\circ$  E), obtained by a meteor radar at a height between 90 and 95 km (Pancheva et al., 2002), showed amplitudes of about 20 m/s in June and July, which correspond to double the values of the zonal components observed at Cariri. On the other hand, the meridional amplitude observed at these sites was very similar. Simultaneous observations at Cariri and Jakarta could answer the question as to whether the difference in the zonal wind amplitudes always exists, or was as a result of the observations taken in different years. Hitchman and Leovy (1986) have reported about the contamination of the wind data by the significantly zonally asymmetric motions at the equator when observed by one site, but a network of radars must be considered to collect simultaneous information about the wind, in order to clarify this problem. According to the model, between 70 and 100 km of height,

April, July and October have amplitudes of both components increasing with height, except for January when the meridional amplitude has its smaller value between 85 and 90 km. Comparing with observed data, the model does not agree with zonal data because, in July, for example, the amplitude presented a maximum zonal amplitude at 88 km and October presented a clear peak at 88–91 km. On the other hand, in January the meridional diurnal amplitude presented a minimum at 91–94 km, which agrees well with the GSWM.

At 82 km, the amplitude of the zonal diurnal tide was weak during the 12 months of observations and no seasonal variation was clear, in contrast to the monthly zonal mean wind where the seasonal variation was strong. At 98 km altitude, the diurnal tidal amplitude presented a strong seasonal variation and the monthly zonal wind did not present a clear 6-month oscillation. The diurnal tides generally present peak amplitudes between 90 and 105 km. The dissipation of the (1,1) mode results in deposition of the western momentum to the mean flow (Andrews and McIntyre, 1978). The meridional diurnal amplitude, on the other hand, presented a clear seasonal variation mainly at 91–98 km of altitude and, on average, it was larger than the zonal diurnal tide, except at 98 km in August–October when the zonal amplitude was  $\sim 40$  m/s. The amplitude maximum in the zonal diurnal tide was observed at Cariri at 98 km. According to Hays et al. (1994), these maxima occur at equinoxes and minima at solstices, between 95 and 100 km, which agree with our observations. We are not able to affirm that 98 km is the region where the amplitude is maximum. If we consider the meridional diurnal amplitude, we could say that the amplitude maxima is around 91–98 km and presents a seasonal behavior. McLandress (2002b), using an extended version of the Canadian Middle Atmospheric Model (CMAM), discusses the effect of the seasonal variation of the mean winds and the effect of solar heating in the near infrared (water vapor), ultraviolet (ozone) and extreme ultraviolet (atomic oxygen), with regards to the semiannual oscillation of diurnal tide.

The temporal series of data (1 yr) used in this work did not permit one to identify a QBO in the wind over Cariri, but future works with longer periods of data could feature the behavior of the upper mesosphere QBO at 7.5 degree south.

## 7 Conclusions

Wind data recorded between July 2004 and June 2005 observed by the meteor radar at Cariri (7.4° S; 36.5° W), Brazil, showed a strong semiannual variation for the zonal background wind component with the largest velocity amplitudes at 82 km and a nearly linear decrease in amplitude with height. The westward wind was strongest in March and September, between 82 and 91 km, whereas a weaker eastward component was present during solstice only at heights between 82 and 91 km. The meridional wind, on the other hand, presented basically an annual variability with a weak

northward component in the summer solstice. The southward component was maximum in winter for all heights from 82 to 98 km. Comparing with the models, we can comment that the CIRA describes very poorly the zonal wind observed at Cariri. This is because winds calculated by CIRA are derived from the thermal wind equation using satellite radiances, which requires geostrophic balance. However, the Coriolis torque is low at the equator, which must make such conversions difficult and prone to errors. On the other hand, for the HWM93 model, both components are in good agreement with the observed wind. The amplitudes of the diurnal and semidiurnal tides of both components, zonal and meridional winds, were also calculated. The meridional diurnal amplitude, on average, was twice the zonal one presented by GSWM. In addition, the meridional phase always presented a smooth variation with height for all months, whereas the zonal diurnal phase showed a large variation with height, so that a vertical wavelength could often not be found for the zonal component. The rotary spectrum has shown that the winds rotate predominately anticlockwise which means that most of the tidal waves propagate upward.

*Acknowledgements.* The authors are grateful to the Coordenacao de Aperfeicoamento de Pessoal de Nivel Superior (CAPES), Conselho Nacional de Desenvolvimento Cientifico e Tecnologico (CNPQ) and Fundacao de Amparo a Pesquisa do Estado de S. Paulo (FAPESP) which supported this research. Also, we wish to thank the Federal University of Campina Grande (UFCG), Federal University of Paraiba (UFPB) and the S. J. do Cariri Prefecture. We are also grateful for suggested improvements provided to the original manuscript by L. Lima.

Topical Editor U.-P. Hoppe thanks D. Pancheva and another anonymous referee for their help in evaluating this paper.

## References

- Andrews, D. G. and McIntyre, M. E.: Generalized Eliassen-Palm and Cherney-Drazin theorems for waves on axisymmetric mean flows and compressible atmospheres, *J. Atmos. Sci.*, 35, 175–185, 1978.
- Batista, P. P., Clemesha, B. R., Tokumoto, A. S., and Lima, L. M.: Structure of the mean winds and tides in the meteor region over Cachoeira Paulista, Brazil (22.7° S, 45° W) and its comparison with models, *J. Atmos. Sol.-Terr. Phys.*, 66(6–9), 623–636, 2004.
- Bevington, R. P.: *Data Reduction and Error Analysis for the Physical Sciences*, McGraw-Hill, 336 pp., 1969.
- Burrage, M. D., Vincent, R. A., Mayr, H. G., Skinner, W. R., Arnold, N. F., and Hays, P. B.: Long-term variability in the equatorial middle atmosphere zonal wind, *J. Geophys. Res.*, 101, 12 847–12 854, 1996.
- Chapman, S. and Lindzen, R. S. *Atmospheric Tides*, Reidel, Dordrecht, 1970.
- Dunkerton, T. J.: On the role of Kelvin wave in the westerly phase of the semiannual zonal wind oscillation, *J. Atmos. Sci.*, 36, 32–41, 1979.
- Dunkerton, T. J.: Theory of the mesopause semiannual oscillation, *J. Atmos. Sci.*, 39, 2681–2690, 1982.

- Fleming, E. L., Chandra, S., Barnett, J. J., and Corney, M.: Zonal mean temperature, pressure, zonal wind and geopotential height as functions of latitude, *Adv. Space Res.*, 10(12), 11–62, 1990.
- Forbes, J. A.: Atmospheric Tides, 1, Model description and results for the solar diurnal components, *J. Geophys. Res.*, 87, 5222–5240, 1982.
- Garcia, R. R., Dukerton, T. J., Lieberman, R. S., and Vincent, R. A.: Climatology of the semiannual oscillation of the tropical middle atmosphere, *J. Geophys. Res.*, 102(D22), 26 019–26 032, 1997.
- Garcia, R. R. and Sassi, F.: Modulation of the mesospheric semi-annual oscillation by the quasi-biennial oscillation, *Earth Planets Space*, 51, 563–569, 1999.
- Geller, M. A., Yudin, V. A., Khattatov, B. V., and Hagan, M. E.: Modeling the diurnal tide with dissipation derived from UARS/HRDI measurements, *Ann. Geophys.*, 15, 1198–1204, 1997, <http://www.ann-geophys.net/15/1198/1997/>.
- Gill, A. E.: *Atmosphere-Ocean Dynamics*, Academic Press, New York, 1982.
- Groves, G. V.: Annual and semi-annual wind components and corresponding temperature and density variations, 60–130 km, *Planet. Space Sci.* 20, 2099–2112, 1972.
- Hagan, M. E. and Forbes, J. M.: Migrating and nonmigrating diurnal tides in the middle and upper atmosphere excited by tropospheric latent heat release, *J. Geophys. Res.*, 107(D24), 4754, doi:10.1029/2001JD001236, 2002.
- Hagan, M. E. and Forbes, J. M.: Migrating and nonmigrating semidiurnal tides in the upper atmosphere excited by tropospheric latent heat release, *J. Geophys. Res.*, 108(A2), 1062, doi:10.1029/2002JA009466, 2003.
- Hays P. B., Wu, D. L., Burrage, M. D., Cell, D. A., Grass, H. J., Lieberman, R. S., Marshall, A. R., Morton, Y. T., Orland, D. A., and Skinner, W. R.: Observations of the diurnal tide from space, *J. Atmos. Sci.*, 51, 3077–3093, 1994.
- Hedin, A. E., Biondi, M. A., Burnside, R. G., Hernandez, G., Johnson, R. M., Killeen, T. L., Mazaudier, C., Meriwether, J. W., Salah, J. E., Sica, R. J., Smith, R. W., Spencer, N. W., Wikwar, V. B., and Virdi, T. S.: Revised Global Model of Thermosphere Winds Using Satellite and Ground-Based Observations, *J. Geophys. Res.*, 96, 7657–7688, 1991.
- Hedin, A. E., Fleming, E. L., Manson, A. H., Schmidlin, F. J., Avery, S. K., Clark, R. R., Franke, S. J., Fraser, G. J., Tsuda, T., Vial, F., and Vincent, R. A.: Empirical wind model for the upper, middle and lower atmosphere, *J. Atmos. Terr. Phys.*, 58, 1421–1447, 1996.
- Hitchman, M. H. and Leovy, C. B.: Evolution of the zonal mean state in the equatorial middle atmosphere during October 1978–May 1979, *J. Atmos. Sci.*, 43, 3159–3176, 1986.
- Hirota, I.: Equatorial waves in the upper stratosphere and mesosphere in relation to the semiannual oscillation of the zonal wind, *J. Atmos. Sci.*, 35, 714–722, 1978.
- Hocking, W. K. and Thayaparan, T.: Simultaneous and co-located observation of winds and tides by MF and meteor radar over London, Canada, (43° N, 81° W) during 1994–1996, *Radio Sci.*, 32, 833–865, 1997.
- Hocking, W. K.: Middle atmosphere dynamical studies at Resolute Bay over a full representative year: Mean winds, tides, and special oscillations, *Radio Sci.*, 36(6), 1795–1822, 2001.
- Hocking, W. K., Fuller, B., and Vandeppeer, B.: Real-time determination of meteor-related parameters utilizing modern digital technology, *J. Atmos. Sol.-Terr. Phys.*, 63(2–3), 155–169, 2001.
- Hocking, W. K., and Hocking, A.: Temperature tides determined with meteor radar, *Ann. Geophys.*, 20, 1447–1467, 2002, <http://www.ann-geophys.net/20/1447/2002/>.
- Labitzke, K., Barnett, J. J., and Edwards, B. (Eds.): *Middle Atmosphere Program, MAP Handbook, Volume 16*, University of Illinois, Urbana, 1985.
- Lieberman, R. S., Burrage, M. D., Gell, D. A., Hays, P. B., Marshall, A. R., Orland, D. A., Skinner, W. R., Wu, D. L., Vincent, R. A., and Franke, S. J.: Zonal mean winds in the equatorial mesosphere and lower thermosphere observed by the High Resolution Doppler Imager, *Geophys. Res. Letts.*, 20, 2849–2852, 1993.
- Manson, A. H., Meek, C. E., Avery, S. K., Fraser, G. J., Vincent, R. A., Phillips, A., Clark, R. R., Schminder, R., Kurschner, D., and Kazimirovski, E. S.: Tidal winds from the mesosphere, lower thermosphere global radar network during the second LTCS campaign, December 1988, *J. Geophys. Res.*, 96, 1117–1127, 1991.
- McLandress, C., Shepherd, G. G., and Solheim, B. H.: Satellite observations of thermospheric tides: Results from the Wind Imaging Interferometer on UARS, *J. Geophys. Res.*, 101, 4093–4114, 1996.
- McLandress, C.: The Seasonal Variation of the Propagating Diurnal Tide in the Mesosphere and Lower Thermosphere. Part I: The Role of Gravity Waves and Planetary Waves, *J. Atmos. Sci.*, 59, 893–906, 2002a.
- McLandress, C.: The Seasonal Variation of the Propagating Diurnal Tide in the Mesosphere and Lower Thermosphere. Part II: The Role of Tidal Heating and Zonal Mean Winds, *J. Atmos. Sci.*, 59, 907–922, 2002b.
- Medeiros, A. F., Takahashi, H., Buriti, R. A., Pinheiro, K. M., and Gobbi, D.: Atmospheric gravity wave propagation direction observed by airglow imaging in the South American sector, *J. Atmos. Sol.-Terr. Phys.*, 67, 1767–1773, 2005.
- O'Brien, J. J. and Pillsbury, R. D.: Rotary wind spectra in a sea breeze regime, *J. Appl. Meteorol.*, 13, 7, 820–825, 1974.
- Oort, A. H.: *Global Atmospheric Circulation Statistics 1958–1983*, National Oceanic and Atmospheric Administration, Professional Paper 14, 180 pp., U.S. Government Printing Office, Washington, D.C., 1983.
- Pancheva, D., Mitchell, N. J., Hagan, M. E., Manson, A. H., Meek, C. E., Luo, Y., Jacobi, Ch., Kurschner, D., Clark, R. R., Hocking, W. K., MacDougall, J., Jones, G. O. L., Vincent, R. A., Reid, I. M., Singer, W., Igarashi, K., Fraser, G. I., Nakamura, T., Tsuda, T., Portnyagin, Y., Merzlyakov, E., Fahrutdinova, A. N., Stepanov, A. M., Poole, L. M. G., Malinga, S. B., Kashcheyev, B. L., Oleynikov, A. N., and Riggan, D. M.: Global-scale tidal structure in the mesosphere and lower thermosphere during the PSMOS campaign of June–August 1999 and comparisons with the global-scale wave model, *J. Atmos. Sol.-Terr. Phys.*, 64, 1011–1035, 2002.
- Pancheva, D., Mitchell, N. J., and Younger, P. T.: Meteor radar observations of atmospheric waves in the equatorial mesosphere/lower thermosphere over Ascension Island, *Ann. Geophys.*, 22, 387–404, 2004, <http://www.ann-geophys.net/22/387/2004/>.
- Rajaram, R. and Gurubaran, S.: Seasonal variabilities of low-latitude mesospheric winds, *Ann. Geophys.*, 16, 197–204, 1998,

- <http://www.ann-geophys.net/16/197/1998/>.
- Reed, R. J.: The quasi-biennial oscillation of the atmosphere between 30 and 50 km over Ascension Island, *J. Atmos. Sci.*, 22, 331–333, 1965.
- Reed, R. J.: Zonal wind behavior in the equatorial stratosphere and lower mesosphere, *J. Geophys. Res.*, 71, 4223–4233, 1966.
- Salby, M. L., Hartmann, D. L., Bailey, P. L., and Gille, J. C.: Evidence for equatorial Kelvin modes in Nimbus 7 LIMS, *J. Atmos. Sci.*, 40, 220–235, 1984.
- Taylor, M. J., and Hapgood, M. A.: Identification of a thunderstorm as a source of short period gravity waves in the upper atmospheric nightglow emission, *Planet. Space Sci.*, 36, 975–985, 1988.
- Vincent, R. A.: Gravity-wave motions in the mesosphere, *J. Atmos. Terr. Phys.*, 46(2), 119–128, 1984.
- Vincent, R. A., Tsuda, T., and Kato, S.: A comparative study of mesospheric solar tides observed at Adelaide and Kyoto, *J. Geophys. Res.*, 93, 699–708, 1988.
- Vincent, R. A.: Long-period motions in the equatorial middle atmosphere, *J. Atmos. Terr. Phys.*, 55, 1067–1080, 1993.
- Wu, D. L., Hays, P. B., and Skinner, W. R.: A Least Squares Method for Spectral Analysis of Space-Time Series, *J. Atmos. Sci.*, 52, 3501–3511, 1995.